CrossMark

ORIGINAL PAPER

Semi-automated echocardiographic quantification of right ventricular size and function

Diego Medvedofsky[1] · Karima Addetia[1] · Jamie Hamilton[2] · Javier Leon Jimenez[3] · Roberto M. Lang[1] · Victor Mor-Avi[1]

Abstract Although parameters of right ventricular (RV) size and function are clinically important, echocardiographic assessment of this chamber is complex. Existing quantitative approaches rely on manual measurements performed on different images, and are thus time-consuming. Consequently, in clinical practice, qualitative assessment is usually used instead. We tested a new approach for automated measurements of RV size and function using speckle tracking by comparing them to the conventional manual methodology. Transthoracic images were obtained in 149 patients with a wide range of RV size and function, and were analyzed by an expert using conventional techniques to obtain RV end-diastolic and end-systolic areas, fractional area change, dimensions (basal and mid-cavity diameters and length), tricuspid annular plane systolic excursion and peak systolic velocity. Same parameters were obtained using the semi-automated software (Epsilon Imaging), which requires tracing of the RV endocardial boundary in a single frame in the RV focused view. Fifteen patients were excluded due to image quality (90 % feasibility). Time required for the automated analysis was approximately 30 s per patient, compared to 4 min for conventional analysis. The parameters obtained with the semi-automated approach were in good agreement with manual measurements: r-values 0.79–0.95 for RV size and 0.70–0.74 for function indices and biases of 2–22 % of the mean measured values, which were comparable to the intrinsic variability of the conventional technique. In conclusion, the semi-automated technique is feasible, fast and provides quantitative parameters of RV size and function, which are comparable to conventional measurements.

Keywords Right ventricle · Ventricular function · Echocardiography · Automated quantification

Introduction

Although parameters of right ventricular (RV) size and function are clinically important, assessment of this chamber is complex. Until recently, RV assessment was qualitative only and thus subjective and experience dependent. The new guidelines from the American Society of Echocardiography have emphasized the importance of quantitative assessment of RV size and function and encouraged making these measurements standard in clinical practice [1]. Previous studies have shown that RV measurements provide important prognostic and therapeutic information in patients with heart disease [2–9]. However, current quantitative approaches rely on manual measurements performed on a variety of images, including endocardial boundary tracings on 2D images for chamber area and dimensions, measurements of tricuspid annular plane systolic excursion (TAPSE) on M-Mode images and tricuspid annular velocity on tissue Doppler images (S'). This methodology is time-consuming and experience dependent. As a result, in clinical practice, visual qualitative assessment of RV size and function is usually used instead, despite the clear benefits of a quantitative assessment. Accordingly, development of new tools for fast, accurate and reproducible measurement of RV indexes would address an important clinical need.

✉ Victor Mor-Avi
vmoravi@bsd.uchicago.edu

1 Section of Cardiology, Department of Medicine, University of Chicago Medical Center, 5841 South Maryland Avenue, MC5084, Chicago, IL 60637, USA

2 Epsilon Imaging, Ann Arbor, MI, USA

3 Jerez de la Frontera Hospital, Cádiz, Spain

Several automated software packages for the evaluation of the left ventricle were developed and tested over the past two decades [10–26], but very little has been published regarding automated analysis of the right ventricle [27–30]. However, new vendor-independent computer software for automated assessment of RV size and function has been recently developed, aimed at facilitating the workflow in busy clinical laboratories and in core laboratories running clinical trials that involve RV measurements. This new software is based on endocardial tracking throughout the cardiac cycle using ultrasound speckle-tracking technology, and is attractive because of its speed and ease of use, as it requires minimal user input. In addition to the traditional indices of RV size and function, the new software also measures RV strain, a novel index of RV function, which has recently been shown useful as a diagnostic tool in a variety of clinical settings.

The aim of this study was to assess the feasibility, accuracy and reproducibility of the new semi-automated software in patients with a wide range of RV size and function, compared to a reference standard of conventional manual measurements.

Methods

We retrospectively identified 149 adult patients with a wide range of RV size and function, who had a clinically indicated transthoracic echocardiogram that included the apical RV focused view. The only predefined echocardiographic exclusion criterion was inadequate quality of the apical RV focused view. In all these patients, comprehensive 2D and Doppler echocardiographic images were acquired by an experienced sonographer using the iE33 imaging system (Philips Healthcare, Andover, MA). The study was approved by the Institutional Review Board of the University of Chicago Medical Center.

Semi-automated image analysis

Digital cine loops of the apical RV-focused views were analyzed using the new dedicated software (EchoInsight, Epsilon Imaging, Ann Arbor, MI) (Fig. 1). The user input consisted of initialization of the RV endocardial border in a single frame (Fig. 1a). The software then performed automated border refinement and tracking throughout the cardiac cycle (Fig. 1b, c). The software provides the user with an opportunity to visually check the endocardial tracking and correct the boundaries if necessary until tracking is judged as accurate. However, in this study, no such adjustments were performed, in order to determine the accuracy of a truly automated analysis.

The software uses the RV endocardial boundaries to quantify RV area throughout the cardiac cycle by automatically tracking intramyocardial speckles frame-by-frame. End-systole was defined by the software as the frame that depicts the smallest RV area. The analysis resulted in a number of conventional quantitative indices of RV size and function, including: end-diastolic area (EDA) (Fig. 1b), end-systolic area (ESA) (Fig. 1c), fractional area change (FAC), RV dimensions (RV basal diameter, RV mid-cavity diameter and RV length) (Fig. 1d), TAPSE [Fig. 1a (red arrow)] and RV basal free-wall segment peak systolic excursion velocity (S').

Reference measurements

The automated measurements were compared with reference values obtained using conventional methodology based on manual measurements (Fig. 2), which were performed according to the recommendations of the American Society of Echocardiography [1]:

- RV ESA and EDA were obtained by tracing the RV endocardium at end-systole and end-diastole from the annulus, along the free wall to the apex, and then back to the annulus, along the interventricular septum (Fig. 2a, b). Care was taken to trace the free wall between the trabeculae and the compacted myocardium.
- RV FAC was defined as (EDA − ESA)/EDA × 100 (in % of EDA).
- RV dimensions (Fig. 2c): The basal diameter was measured as the maximal short-axis dimension in the basal one-third of the right ventricle seen on the 4-chamber view. The mid-cavity diameter was measured in the middle one-third of the right ventricle at the level of the papillary muscles. The longitudinal dimension was drawn from the plane of the tricuspid annulus to the RV apex.
- TAPSE was measured by placing an M-mode cursor through the tricuspid annulus and measuring the amplitude of longitudinal motion of the annulus in systole (Fig. 2d).
- S' was measured using pulsed tissue Doppler imaging (systolic excursion velocity) in an apical 4-chamber view highlighting the RV free wall with the sample volume placed on the free-wall side of the tricuspid annulus. To minimize the effects of noise in the velocity curves, peak velocity was measured in the middle of the Doppler tracing (Fig. 2e).

Reproducibility analysis

Both semi-automated and manual measurements were repeated in a randomly selected subgroup of 30 patients by two experienced readers for purposes of reproducibility analysis. This included repeated measurements by the same observer, at least 1 month later, as well as measurements
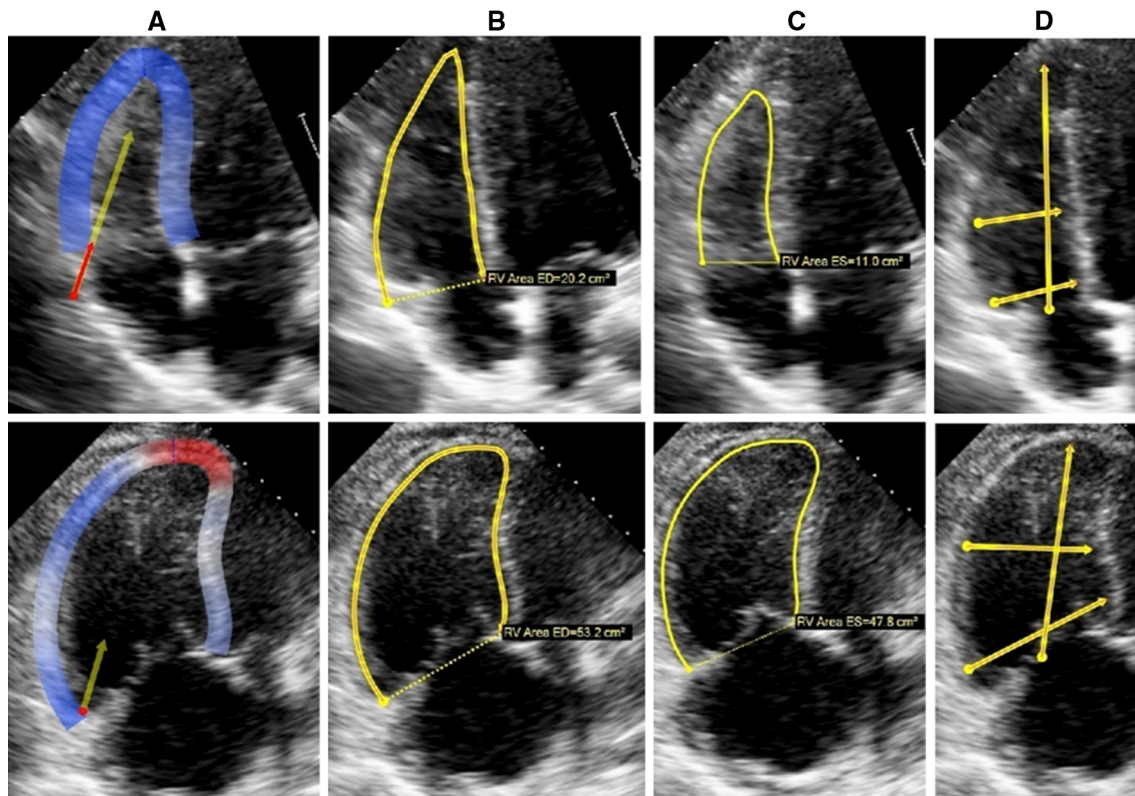
Fig. 1 New software for automated analysis of RV size and function in a normal subject (*top*) and a patient with RV pressure and volume overload (*bottom*). After manual initialization of the RV boundaries (**a**), and automated tracking throughout the cardiac cycle, end-diastolic and end-systolic area automatically measured (**b** and **c**), as

well as end-diastolic RV dimensions, including RV length, and basal and mid-cavity diameters (**d**, *arrows*). In addition, RV function parameters are automatically measured, including TAPSE (**a** direction shown as a *yellow arrow* and amplitude shown as a *red arrow*) and RV basal free-wall segment S' velocity

by a second independent observer, both blinded to all prior measurements. Inter-observer and intra-observer variability were calculated as an absolute difference between the corresponding pair of repeated measurements as a percentage of their mean in each patient and then averaged over the entire study group.

Statistical analysis

Data were expressed as mean ± SD for descriptive statistics. Inter-technique comparisons included linear regression with Pearson's correlation and Bland–Altman analyses to assess the bias and limits of agreement with the reference technique. The calculated biases were compared with the intrinsic variability of the manual reference technique in order to better appreciate the level of inter-technique agreement.

Results

Automated analysis of RV size and function was feasible in 134 of 149 patients (90 %). The remaining 15 patients were excluded because of suboptimal apical RV focused views

(10 %). Of the 134 patients, 38 were males, mean age was 56 ± 17 years, and BSA was 1.82 ± 0.24 m^2. Time required for the automated analysis was approximately 30 s per patient on a standard personal computer, compared to approximately 4 min required for the conventional analysis.

Table 1 shows the summary of the RV size and function indices measured by the conventional manual and the automated techniques, as well as the results of the inter-technique comparisons, including correlation coefficients, and Bland–Altman analysis derived mean inter-technique differences (biases) with the corresponding SDs. In addition, biases and SDs in percent of the mean of the two measurements are listed (Table 1, right column), to allow comparisons with the intrinsic variability of each parameter when measured using the conventional methodology.

Linear regression showed good inter-technique correlation between RV size parameters (areas and dimensions), as reflected by r-values in the range of 0.79–0.95 (Fig. 3, top left and middle; Fig. 4, top), and lower but still good correlations between RV function parameters (FAC, TAPSE and S') with r-values between 0.70 and 0.74 (Fig. 3, top right; Fig. 5, top).
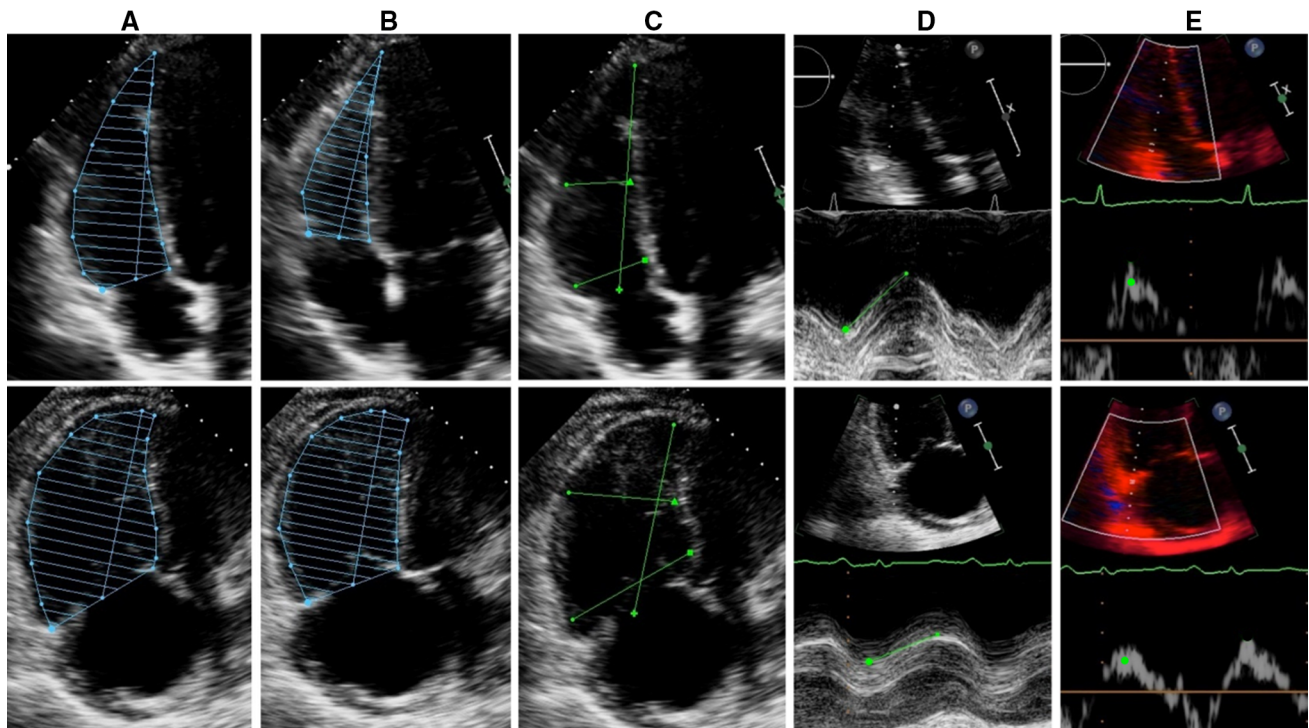
Fig. 2 Reference 2D conventional measurements of RV size and function in a normal subject (*top*) and a patient with RV pressure and volume overload (*bottom*), including end-diastolic and end-systolic areas (**a** and **b**), end-diastolic RV dimensions, including RV length, and basal and mid-cavity diameters (**c**), TAPSE (**d**) and RV basal free-wall segment S' peak velocity by tissue Doppler imaging (**e**), which was measured in the middle of the Doppler tracing to minimize the effects of noise (*green dots*)

Table 1 RV size and function measurements by manual and automated analysis and inter-technique agreement (N = 134)

|	2D conventional	2D automated	Correlation (r-value)	Bias ± SD	Bias (% mean) ± SD
EDA (cm^2)	28 ± 12	31 ± 14	0.94	3.3 ± 5.1	11 ± 16
ESA (cm^2)	20 ± 11	24 ± 13	0.95	4.1 ± 4.3	17 ± 18
FAC (%)	33 ± 12	27 ± 11	0.74	−5.6 ± 8.4	−21 ± 31
RV basal diameter (cm)	4.7 ± 1.1	4.5 ± 1.0	0.79	−0.2 ± 0.7	−4 ± 16
RV mid-cavity diameter (cm)	3.6 ± 1.2	4.6 ± 1.2	0.86	1.0 ± 0.6	22 ± 14
RV length (cm)	8.1 ± 1.2	7.7 ± 1.3	0.86	−0.3 ± 0.7	−4 ± 9
TAPSE (cm)	1.8 ± 0.6	1.6 ± 0.6	0.70	−0.1 ± 0.5	−9 ± 29
S' (cm/sec)	9.4 ± 3.7	9.2 ± 3.9	0.73	−0.21 ± 2.8	−2 ± 30

EDA end diastolic area, *ESA* end systolic area, *FAC* fractional area change, *RV* right ventricle, *TAPSE* tricuspid annular plane systolic excursion, *S'* RV basal free wall segment systolic excursion velocity

Bland–Altman analysis showed that the automated technique overestimated both end-diastolic and end-systolic areas (Fig. 3, bottom left and middle) with small biases (3.3 and 4.1 cm^2, respectively), corresponding to 11 and 17 % of the mean measured area. Importantly, the 95 % limits of agreement (±2 SD of the mean difference) were relatively narrow (−7 to 13 cm^2 for EDA and −5 to 13 cm^2 for ESA). Fractional area change measured by the new system was underestimated (Fig. 3, bottom right) with a bias of 5.6 %, corresponding to 21 % of the mean measured FAC value. The limits of agreement were relatively wide (−22 to

+11 %). The RV dimensions (basal diameter, mid-cavity diameter and longitudinal length) showed biases of −0.2, 1.0 and −0.3 cm, respectively, and reasonably narrow limits of agreement: −1.6 to +1.2 cm, −0.3 to +2.3 cm, −1.6 to +1.1 cm, respectively (Fig. 4, bottom). TAPSE showed a bias of −0.14 cm and limits of agreement from −1.1 to +0.8 cm, while S' showed a bias of −0.21 cm/s with limits of agreement from −5.8 to +5.7 cm/s (Fig. 5, bottom).

The magnitude of the inter-technique biases in percentage of the measured values ranged between 4 and 22 %. The lowest percent errors were noted for S' (2 %),
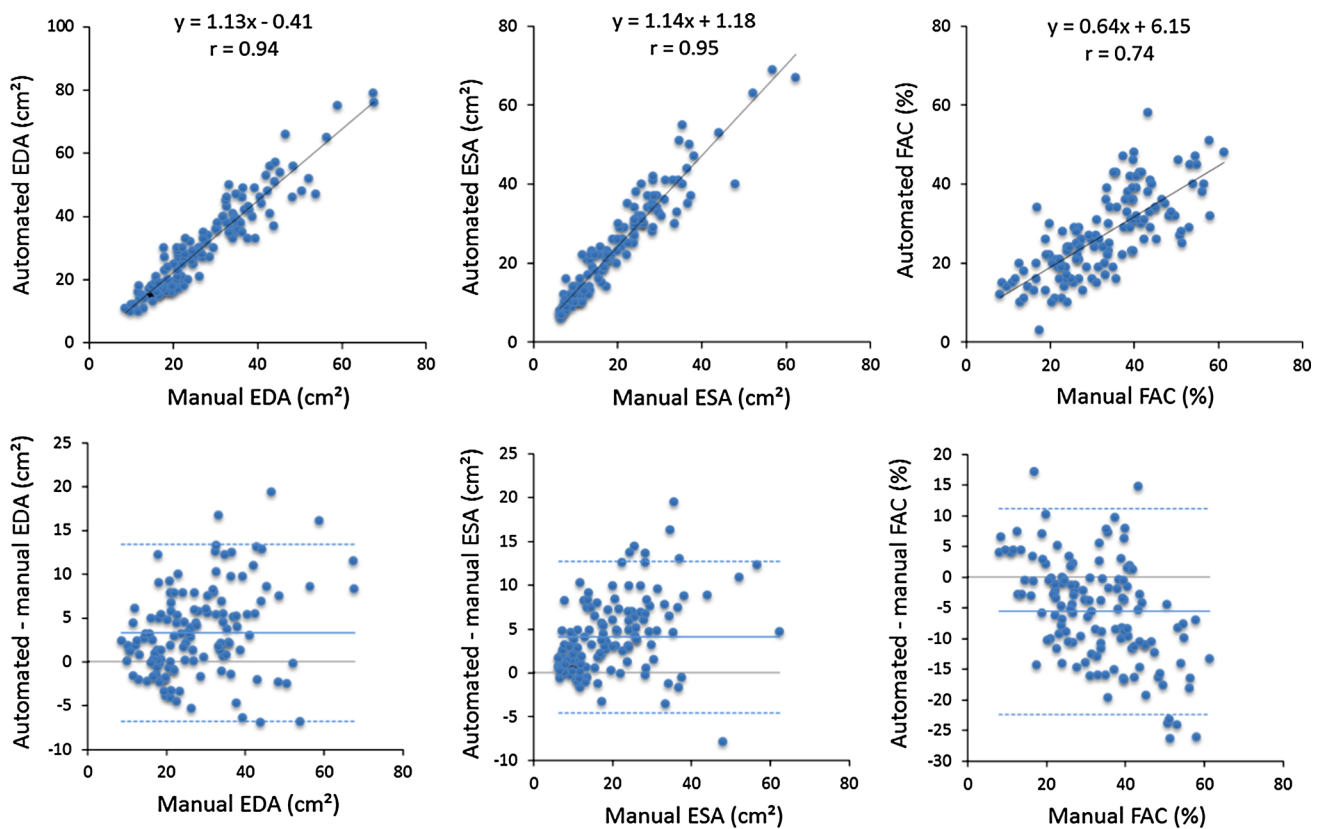
Fig. 3 Results of linear regression (*top*) and Bland–Altman (*bottom*) analyses for EDA (*left*), ESA (*center*) and FAC (*right*) between the automated and conventional manual RV measurements

while FAC and mid-cavity diameter showed the highest biases (21 and 22 %, respectively).

Table 2 shows the results of the reproducibility analysis for EDA, ESA, FAC, Basal RV diameter, mid-cavity RV diameter, RV length, TAPSE and S' for conventional 2DE and the automated software. Not surprisingly, for both techniques, the inter-observer variability was higher than the intra-observer variability for most indices. Importantly, both intra-observer and inter-observer variability for the conventional 2DE technique were higher than for new semi-automated software for most parameters. Of note, both inter- and intra-observer variability of the conventional 2DE measurements were higher than the biases between the new automated technique and the conventional reference, when expressed in % of the measured values (Table 1, right column), indicating that the automated measurements were well within the boundaries of the intrinsic variability of the conventional reference technique.

Discussion

Because the shape of the left ventricle is axially symmetrical, it is possible to model the 3D shape of this chamber using simple geometric assumptions and thus obtain accurate and reproducible measurements from 2D cross-sectional planes, provided that non-foreshortened views are available. In contrast, assessment of RV size and function is more challenging because this chamber has a complex 3D shape without clear axial symmetry and is thus difficult to model. This geometry is further complicated by the wider range of RV loading conditions and greater heterogeneity in its regional function. As a result, there is not a single generally accepted method for assessing RV size and function because each technique has its own limitations. Accordingly, multiple parameters are used in each patient, as surrogate measures of RV function, resulting in a rather cumbersome acquisition and measurement protocols requiring different views and imaging techniques. Consequently, routine clinical assessment of RV size and function is usually qualitative, and may thus be less accurate when performed by less experienced readers.

The goal of this study was to validate a new technique for automated RV assessment, which has the potential to allow routine quantitative evaluation. With this technique, the only manual input is initial tracing of the RV boundaries in a single frame, after which the software automatically traces the RV endocardial border and directly measures a number of RV size and function parameters,
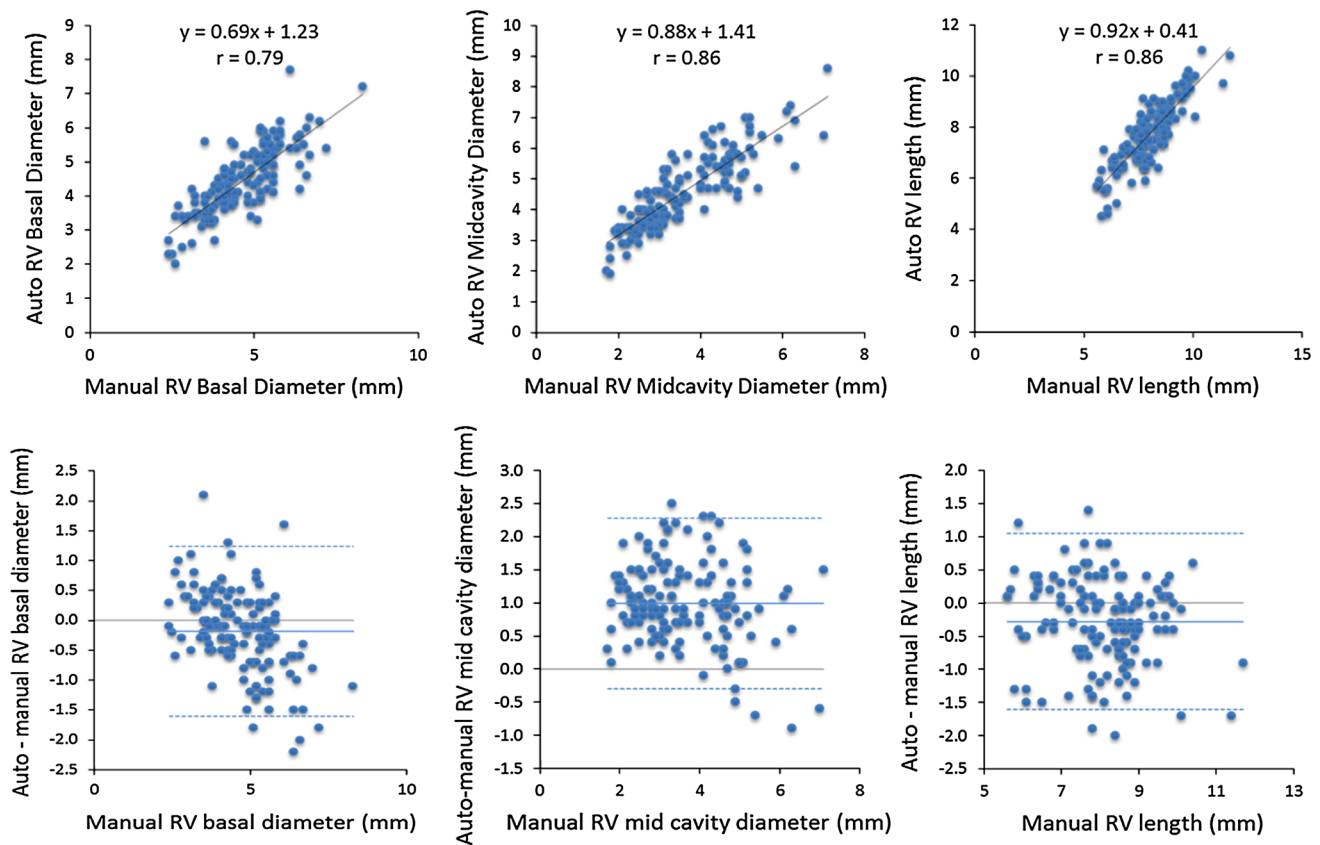
Fig. 4 Results of linear regression (*top*) and Bland–Altman (*bottom*) analyses for RV basal diameter (*left*), RV mid-cavity diameter (*center*) and RV longitudinal length (*right*) between the automated and conventional manual RV measurements

including EDA, ESA, FAC, dimensions (basal and mid-cavity diameters and length), TAPSE and S'. To achieve this goal, we studied 134 patients with a wide range of RV characteristics, in whom different RV size and function parameters were compared between the new semi-automated and conventional reference techniques based on manual measurements.

Our results showed that the new semi-automated technique is feasible in the majority of patients, fast and easy to use, compared to the conventional manual methodology. Using the new technique, we obtained accurate and objective measurements of the RV size and function parameters (Table 1). We found good inter-technique correlations between RV size parameters (areas and dimensions), and lower but still clinically useful correlations between RV function parameters (FAC, TAPSE and S'). The semi-automated technique overestimated both end-diastolic and end-systolic areas with small biases and relatively narrow limits of agreement. The RV basal diameter and length showed small biases and reasonably narrow limits of agreement. The mid-cavity RV diameter measurements showed lower level of inter-technique agreement, probably because of the lack of a globally accepted definition of where it should be measured, beyond

what is specified in the RV guidelines as "measured in the middle third of the right ventricle at the level of the LV papillary muscles" [1]. FAC measured by the new algorithm was underestimated with a bias that was larger, probably as a result of compounding of errors in the calculation of FAC from EDA and ESA. Both TAPSE and S' showed small biases and reasonably narrow limits of agreement.

Moreover, we found that the reproducibility of this new technique was better than that of the conventional manual methodology (Table 2). This is not unexpected because of the largely automated nature of this new software, wherein the only source of inter-measurement variability is the manual initialization of the endocardial boundary. Importantly, the reproducibility of the mid-cavity diameter, which was apparently the least accurate among all RV size parameters, was better for the automated technique. This is probably because the automated technique is more consistent in the identification of this measurement, whereas the conventional manual technique relies on the individual reader's determination of correct location for this measurement. The relatively wide variability in automated S' measurements probably reflects the sensitivity of this measurement to minor variations in the initial tracing of all

Fig. 5 Results of linear regression (*top*) and Bland–Altman (*bottom*) analyses for TAPSE (*left*) and S' (*right*) between the automated and conventional manual RV measurements
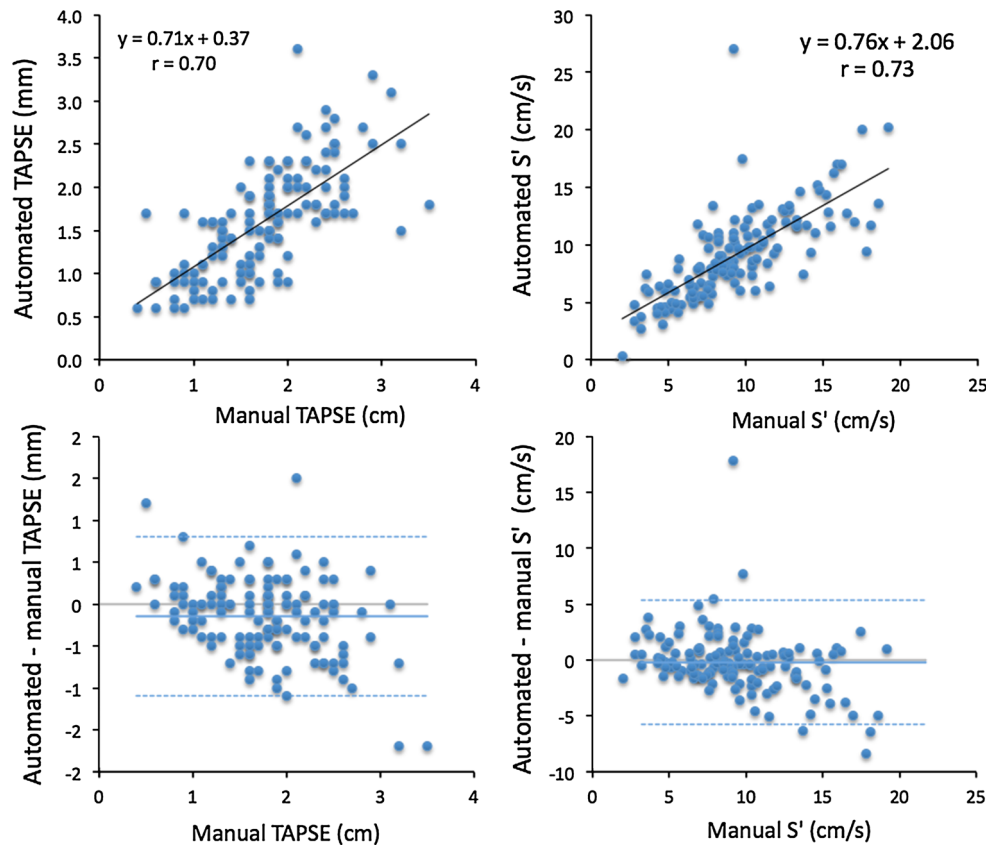
the endocardial boundaries in the RV focused view, compared to the conventional technique that derives this parameter from pulsed tissue Doppler signal.

Because the conventional RV assessment has its own inter-measurement variability, when comparing a new technique to this imperfect reference, one cannot expect a perfect inter-technique agreement. However, the differences between RV parameters obtained using the new semi-automated software and the conventional measurements were smaller than the intrinsic variability of the conventional measurements. This finding supports the notion that the semi-automated assessment is indeed accurate compared to the manual reference.

This new technique also reports global and segmental free-wall longitudinal RV strain values. Strain is a measure of deformation that is the basic descriptor of both the nature and the function of cardiac tissue. Strain analysis by echocardiography involves tracking features of the myocardial texture in consecutive images, which is known as speckle tracking and allows estimation of in-plane myocardial motion and deformation in two dimensions. Speckle tracking is today widely accepted in the context of functional assessment of the left ventricle. In the last few years, there has been increasing interest in the use of this technique for RV analysis [31–38]. Compared to other markers of function, strain measurements have been reported to be angle-independent, less load-

sensitive and able to accurately reflect regional deformation. Thus it has the potential to address each of the major limitations to RV quantification and provide the much needed, objective, inexpensive and relatively simple measure of RV function. In this study, strain measurements could not be compared to a widely accepted independent reference, because such a reference does not yet exist [39].

One limitation of the new automated RV assessment software is that it requires manual tracing of the RV boundaries at one time in the cardiac cycle, which depends on image quality and can be reasonably expected to yield inaccurate measurements in patient with suboptimal acoustic windows. Another limitation of this approach is that it remains intrinsically two-dimensional and does not take advantage of the recent technological advances in real-time 3D echocardiography, which offer accurate measurements of RV volumes and ejection fraction [40–45]. However, 3D imaging equipment and expertise necessary for 3D analysis of RV size and function are not universally available, and 2D techniques, such as this one, may prove as a useful practical alternative.

A limitation of our study is its retrospective nature, since we used all patients in our clinical database who had RV-focused apical 4-chamber views. Since these images were not specifically acquired for the purposes of this study, it is likely that in a prospective study, a higher percentage of images would be of optimal quality. In addition, one may

Table 2 Reproducibility of RV size and function measurements using conventional manual and the automated techniques

Technique	Intra-observer (%)	Inter-observer (%)
EDA (cm^2)		
Manual	18 ± 10	29 ± 11
Automated	15 ± 13	13 ± 11
ESA (cm^2)		
Manual	22 ± 13	29 ± 11
Automated	17 ± 14	16 ± 12
FAC (%)		
Manual	21 ± 17	21 ± 18
Automated	11 ± 11	19 ± 33
Basal RV diameter (cm)		
Manual	11 ± 6	16 ± 6
Automated	9 ± 8	12 ± 11
Mid-cavity RV diameter (cm)		
Manual	11 ± 8	23 ± 11
Automated	10 ± 7	11 ± 10
Length (cm)		
Manual	9 ± 6	12 ± 6
Automated	10 ± 9	7 ± 4
TAPSE (cm)		
Manual	16 ± 14	17 ± 15
Automated	14 ± 18	15 ± 16
S' (cm/sec)		
Manual	8 ± 8	9 ± 9
Automated	12 ± 14	10 ± 12

EDA end diastolic area, *ESA* end systolic area, *FAC* fractional area change, *RV* right ventricle, *TAPSE* tricuspid annular plane systolic excursion, *S'* RV basal free wall segment systolic excursion velocity

see as a limitation of this study the fact that measurements were compared to reference values derived from the same ultrasound images, as opposed to a completely independent reference obtained by using a different imaging modality. Such independent validation needs to be performed in future studies.

In summary, we tested one of the first nearly automated techniques for echocardiographic assessment of RV size and function. This technique is feasible in the majority of unselected patients, and provides accurate and reproducible quantitative measurements without relying on reader's experience. Accordingly, this technique is well suited for routine use in busy clinical laboratories, pending further validation.

References

1. Rudski LG, Lai WW, Afilalo J, Hua L, Handschumacher MD, Chandrasekaran K et al (2010) Guidelines for the echocardiographic assessment of the right heart in adults: a report from the American Society of Echocardiography endorsed by the European Association of Echocardiography, a registered branch of the European Society of Cardiology, and the Canadian Society of Echocardiography. J Am Soc Echocardiogr 23:685–713 **quiz 86-8**
2. Saguner AM, Vecchiati A, Baldinger SH, Rueger S, Medeiros-Domingo A, Mueller-Burri AS et al (2014) Different prognostic value of functional right ventricular parameters in arrhythmogenic right ventricular cardiomyopathy/dysplasia. Circ Cardiovasc Imaging 7:230–239
3. Cohen S, Gaddam S, Gemignani A, Wu WC, Sharma S, Choudhary G (2013) Right ventricular function relates to functional capacity in men with atrial fibrillation and preserved left ventricular ejection fraction. Echocardiography 30:542–550
4. Leong DP, Hoke U, Delgado V, Auger D, Witkowski T, Thijssen J et al (2013) Right ventricular function and survival following cardiac resynchronisation therapy. Heart 99:722–728
5. Poliacikova P, Cockburn J, Pareek N, James R, Lee L, Trivedi U et al (2013) Prognostic impact of pre-existing right ventricular dysfunction on the outcome of transcatheter aortic valve implantation. J Invasive Cardiol 25:142–145
6. Damy T, Ghio S, Rigby AS, Hittinger L, Jacobs S, Leyva F et al (2013) Interplay between right ventricular function and cardiac resynchronization therapy: an analysis of the CARE-HF trial (Cardiac Resynchronization-Heart Failure). J Am Coll Cardiol 61:2153–2160
7. Guazzi M, Bandera F, Pelissero G, Castelvecchio S, Menicanti L, Ghio S et al (2013) Tricuspid annular plane systolic excursion and pulmonary arterial systolic pressure relationship in heart failure: an index of right ventricular contractile function and prognosis. Am J Physiol Heart Circ Physiol 305:H1373–H1381
8. Finocchiaro G, Knowles JW, Pavlovic A, Perez M, Magavern E, Sinagra G et al (2014) Prevalence and clinical correlates of right ventricular dysfunction in patients with hypertrophic cardiomyopathy. Am J Cardiol 113:361–367
9. Pruszczyk P, Goliszek S, Lichodziejewska B, Kostrubiec M, Ciurzynski M, Kurnicka K et al (2014) Prognostic value of echocardiography in normotensive patients with acute pulmonary embolism. JACC Cardiovasc Imaging 7:553–560
10. Perez JE, Waggoner AD, Barzilai B, Melton HE Jr, Miller JG, Sobel BE (1992) On-line assessment of ventricular function by automatic boundary detection and ultrasonic backscatter imaging. J Am Coll Cardiol 19:313–320
11. Michalis LK, Thomas MR, Jewitt DE, Monaghan MJ (1995) Echocardiographic assessment of systolic and diastolic left ventricular function using an automatic boundary detection system. Correlation with established invasive and non invasive parameters. Int J Card Imaging 11:71–80
12. Sapin PM, Kwan OL, Xie GY, Smith MD, DeMaria AN (1995) The assessment of left ventricular filling dynamics using an on-line automatic border detection algorithm: comparison with cineventriculography. Echocardiography 12:559–569
13. Yagi T, Yoshida K, Hozumi T, Akasaka T, Takagi T, Yamamuro A et al (1996) Automatic assessment of left ventricular cavity area by the automated contour tracking method. J Cardiol 28:345–348
14. Iwase M, Kondo T, Hasegawa K, Kimura M, Matsuyama H, Watanabe Y et al (1997) Three-dimensional echocardiography by semi-automatic border detection in assessment of left ventricular volume and ejection fraction: comparison with magnetic resonance imaging. J Cardiol 30:97–105

15. Tighe DA, Paul JJ, Pohl CA, Cook JR, Huhta JC (1998) Automatic border detection for assessment of left ventricular diastolic function among normal neonates: comparison with doppler echocardiography. Echocardiography 15:545–552

16. Jacobs LD, Salgo IS, Goonewardena S, Weinert L, Coon P, Bardo D et al (2006) Rapid online quantification of left ventricular volume from real-time three-dimensional echocardiographic data. Eur Heart J 27:460–468

17. Kirkpatrick JN, Lang RM, Fedson SE, Anderson AS, Bednarz J, Spencer KT (2005) Automated border detection on contrast enhanced echocardiographic images. Int J Cardiol 103:164–167

18. Mele D, Teoli R, Cittanti C, Pasanisi G, Guardigli G, Levine RA et al (2004) Assessment of left ventricular volume and function by integration of simplified 3D echocardiography, tissue harmonic imaging and automated extraction of endocardial borders. Int J Cardiovasc Imaging 20:191–202

19. Rahmouni HW, Ky B, Plappert T, Duffy K, Wiegers SE, Ferrari VA et al (2008) Clinical utility of automated assessment of left ventricular ejection fraction using artificial intelligence-assisted border detection. Am Heart J 155:562–570

20. Sugioka K, Hozumi T, Watanabe H, Yamagishi H, Matsumura Y, Takemoto Y et al (2003) Rapid and accurate noninvasive assessment of global left ventricular systolic function using biplane advanced automated contour tracking method. J Am Soc Echocardiogr 16:1237–1243

21. Sugioka K, Hozumi T, Yagi T, Yamamuro A, Akasaka T, Takeuchi K et al (2003) Automated quantification of left ventricular function by the automated contour tracking method. Echocardiography 20:313–318

22. Rein AJ, Tracey M, Colan SD, Pollak A, Sanders SP (1998) Automated left ventricular endocardial border detection using acoustic quantification in children. Echocardiography 15:111–120

23. Kanzaki Y, Yoshida K, Hozumi T, Akasaka T, Takagi T, Yonezawa Y et al (1999) Measurement of left ventricular filling by automated contour tracking method in echocardiography: comparison with radionuclide ventriculography. J Cardiol 34:207–210

24. Grandi AM, Bignotti M, Bertolini A, Gaudio G, Zanzi P, Guasti L et al (1997) Clinical feasibility of echocardiographic automated border detection in monitoring left ventricular response to acute changes of preload in normal subjects. Cardiology 88:393–396

25. Mor-Avi V, Gillesberg IE, Korcarz C, Sandelski J, Lang RM (1995) Improved quantification of left ventricular function by applying signal averaging to echocardiographic acoustic quantification. J Am Soc Echocardiogr 8:679–689

26. Morrissey RL, Siu SC, Guerrero JL, Newell JB, Weyman AE, Picard MH (1994) Automated assessment of ventricular volume and function by echocardiography: validation of automated border detection. J Am Soc Echocardiogr 7:107–115

27. Oe M, Gorcsan J 3rd, Mandarino WA, Kawai A, Griffith BP, Kormos RL (1995) Automated echocardiographic measures of right ventricular area as an index of volume and end-systolic pressure-area relations to assess right ventricular function. Circulation 92:1026–1033

28. Forni G, Pozzoli M, Cannizzaro G, Traversi E, Calsamiglia G, Rossi D et al (1996) Assessment of right ventricular function in patients with congestive heart failure by echocardiographic automated boundary detection. Am J Cardiol 78:1317–1321

29. Helbing WA, Bosch HG, Maliepaard C, Zwinderman KH, Rebergen SA, Ottenkamp J et al (1997) On-line automated border detection for echocardiographic quantification of right ventricular size and function in children. Pediatr Cardiol 18:261–269

30. Greiner S, Andre F, Heimisch M, Hess A, Steen H, Katus HA et al (2013) Non-invasive quantification of right ventricular systolic function by echocardiography: a new semi-automated approach. Clin Res Cardiol 102:229–235

31. Chang WT, Tsai WC, Liu YW, Lee CH, Liu PY, Chen JY et al (2014) Changes in right ventricular free wall strain in patients with coronary artery disease involving the right coronary artery. J Am Soc Echocardiogr 27:230–238

32. Marston N, Brown JP, Olson N, Auger WR, Madani MM, Wong D, et al (2014) Right ventricular strain before and after pulmonary thromboendarterectomy in patients with chronic thromboembolic pulmonary hypertension. Echocardiography. doi:10.1111/echo.12812

33. Motoki H, Borowski AG, Shrestha K, Hu B, Kusunose K, Troughton RW et al (2014) Right ventricular global longitudinal strain provides prognostic value incremental to left ventricular ejection fraction in patients with heart failure. J Am Soc Echocardiogr 27:726–732

34. Naderi N, Ojaghi Haghighi Z, Amin A, Naghashzadeh F, Bakhshandeh H, Taghavi S et al (2013) Utility of right ventricular strain imaging in predicting pulmonary vascular resistance in patients with pulmonary hypertension. Congest Heart Fail 19:116–122

35. Okumura K, Humpl T, Dragulescu A, Mertens L, Friedberg MK (2014) Longitudinal assessment of right ventricular myocardial strain in relation to transplant-free survival in children with idiopathic pulmonary hypertension. J Am Soc Echocardiogr 27:1344–1351

36. Platz E, Hassanein AH, Shah A, Goldhaber SZ, Solomon SD (2012) Regional right ventricular strain pattern in patients with acute pulmonary embolism. Echocardiography 29:464–470

37. Rajagopal S, Forsha DE, Risum N, Hornik CP, Poms AD, Fortin TA et al (2014) Comprehensive assessment of right ventricular function in patients with pulmonary hypertension with global longitudinal peak systolic strain derived from multiple right ventricular views. J Am Soc Echocardiogr 27(657–65):e3

38. Ternacle J, Berry M, Cognet T, Kloeckner M, Damy T, Monin JL et al (2013) Prognostic value of right ventricular two-dimensional global strain in patients referred for cardiac surgery. J Am Soc Echocardiogr 26:721–726

39. Fine NM, Chen L, Bastiansen PM, Frantz RP, Pellikka PA, Oh JK, et al (2015) Reference values for right ventricular strain in patients without cardiopulmonary disease: a prospective evaluation and meta-analysis. Echocardiography 32:787–796

40. Shiota T, Jones M, Chikada M, Fleishman CE, Castellucci JB, Cotter B et al (1998) Real-time three-dimensional echocardiography for determining right ventricular stroke volume in an animal model of chronic right ventricular volume overload. Circulation 97:1897–1900

41. Niemann PS, Pinho L, Balbach T, Galuschky C, Blankenhagen M, Silberbach M et al (2007) Anatomically oriented right ventricular volume measurements with dynamic three-dimensional echocardiography validated by 3-Tesla magnetic resonance imaging. J Am Coll Cardiol 50:1668–1676

42. D'Andrea A, Riegler L, Morra S, Scarafile R, Salerno G, Cocchia R et al (2012) Right ventricular morphology and function in top-level athletes: a three-dimensional echocardiographic study. J Am Soc Echocardiogr 25:1268–1276

43. Maffessanti F, Muraru D, Esposto R, Gripari P, Ermacora D, Santoro C et al (2013) Age-, body size-, and sex-specific reference values for right ventricular volumes and ejection fraction by three-dimensional echocardiography: a multicenter echocardiographic study in 507 healthy volunteers. Circ Cardiovasc Imaging 6:700–710

44. Zhang QB, Sun JP, Gao RF, Lee AP, Feng YL, Liu XR et al (2013) Feasibility of single-beat full-volume capture real-time three-dimensional echocardiography for quantification of right ventricular volume: validation by cardiac magnetic resonance imaging. Int J Cardiol 168:3991–3995

45. Renella P, Marx GR, Zhou J, Gauvreau K, Geva T (2014) Feasibility and reproducibility of three-dimensional echocardiographic assessment of right ventricular size and function in pediatric patients. J Am Soc Echocardiogr 27:903–910